Journal of
Materials Chemistry B

Accepted Manuscript

This article can be cited before page numbers have been issued, to do this please use: Y. Liu, F. Meng, J. Nie, J. Niu, X. Yu and W. Lin, *J. Mater. Chem. B*, 2017, DOI: 10.1039/C7TB00979H.

ROYAL SOCIETY OF CHEMISTRY

rsc.li/materials-b

View Article Online
DOI: 10.1039/C7TB00979H

Journal Name

ARTICLE

Two-photon fluorescent probe for detecting cell membranal liquid-ordered phase by an aggregate fluorescence method†

Received 00th January 20xx,
Accepted 00th January 20xx

DOI: 10.1039/x0xx00000x

www.rsc.org/

Yong Liu,[a] Fangfang Meng,[a] Jing Nie,[c] Jie Niu [a] Xiaoqiang Yu[b,] * and Weiying Lin[a,] *

Cell membranal liquid-ordered (Lo) phase controlled structure and function of the cell membranes. In this work, we have engineered a novel two-photon (TP) fluorescent probe, **TP-HVC18**, which remarkably displayed two different fluorescence emission profiles to the aggregate and solution states in the distinct polar environments. In accordance with its aggregate fluorescence, **TP-HVC18** also can emit a red fluorescence signal in Lo phase vesicles. Taking advantage of this unique feature, we have demonstrated that the new TP probe **TP-HVC18** is suitable for imaging membranal Lo phase by an aggregate fluorescence method. Furthermore, the robust probe also exhibited uncontinuous red fluorescence distribution in the cell membranal Lo phase. Based on this intriguing character, we also successfully showed that the novel probe can be employed to exhibit uncontinuous distribution of cell membranal Lo phase by 3D imaging technique. We expect that this aggregation-based fluorescent platform may be extended for the development of a wide variety of TP fluorescent probes for detecting many biological species.

Introduction

Conventional fluorescent dyes have made great contributions to understand luminescence processes of dyes at the molecular level.[1-3] The conclusions drawn from the dilute solution data, however, cannot commonly be extended to the concentrated solutions. Appearance of aggregation-induced emission dyes expand research scope of fluorescent materials.[4] It is found that fluorescent materials with aggregate fluorescence property exhibit great advantages in biological applications,[5-7] including high fluorescence quantum yields, good photostability and low signal to noise ratio.[8] Herein, we have developed a novel fluorescent dye for labeling cell membranal phase state by an aggregate fluorescence method.

Two-photon (TP) dyes were initially employed to image intracellular targets by fluorescence microscopy in 1990.[9] TP technique is an indispensable imaging method in light of its useful applications in some fields such as localized release of bioactive species, photodynamic therapy, optical power limiting, and microfabrication.[10, 11] To facilitate the applications of TP in biomedical research field, constructing a novel TP probe with excellent TP properties is very important.

The cell membranes display a tremendous complexity of constituents including various lipids, carbohydrates, and proteins to accurately coordinate its biological function.[12-16] Cell membranal liquid-ordered (Lo) phase (also called lipid rafts) was discovered by Singer and Nicolson in 1972.[17] It plays a critical role in various biological processes.[18-20] For instance, Lo phase is associated with biological process including the formation of proteins clusters, signal transduction, apoptosis, cell adhesion and migration, synaptic transmission, organization of the cytoskeleton, protein sorting during both exocytosis and endocytosis, and virus invasion. The structure and function of cell plasma membranes have been controlled by cell membranal Lo phases.[21] Thus, to understand of cell membranal function in biology, it is crucial to visualize Lo phase. In the past few years, fluorescent probes have become powerful tools for sensing cell membranes and membranal targets in biological imaging fields.[22-25] Lo phases have been widely investigated by diverse methods, including dynamic simulations, detergent resistance experiments, mass spectrometry analysis, atom force microscopy and fluorescent probes technique.[26] However, up to present, there have been no reports on fluorescent probes with unique properties for sensing cell membranal Lo phase by an aggregate fluorescence method. Thus, developing TP fluorescent probes for sensing cell membranal Lo phases by an aggregate fluorescence method is of high interest.

As TP fluorescence is more favorable than one-photon (OP) fluorescence for biological applications,[27-29] we selected the 2,7-position substituted carbazole derivative as the TP platform. Based on this TP platform , we have developed a novel TP fluorescent probe **TP-HVC18** (Fig. 1). It was found that TP dye **TP-HVC18**

[a] *Institute of Fluorescent Probes for Biological Imaging, School of Chemistry and Chemical Engineering, School of Materials Science and Engineering, University of Jinan, Shandong 250022, P.R. China. E-mail: weiyinglin2013@163.com.*

[b] *Center of Bio & Micro/Nano Functional Materials, State Key Laboratory of Crystal Materials, Shandong University, Jinan, 250100, P. R. China.*

E-mail: yuxq@sdu.edu.cn

[c] *School of Chemical Engineering & Technology, China University of Mining and Technology, Xuzhou, Jiangsu, 221116, P.R. China.*

† Electronic Supplementary Information (ESI) available: Experimental details including synthesis, the characterization of the compounds, fluorescence spectroscopic data, and living cells imaging. See DOI: 10.1039/x0xx00000x.

containing long hydrophobic chains could display two different fluorescence emission profiles to the aggregate and solution states in the distinct polar environments. In accordance with its optical properties in the aggregation state, **TP-HVC18** also can emit a red fluorescence signal in Lo phase vesicles. View of this unique property, the novel TP dye **TP-HVC18** was capable of imaging membranal Lo phase by an aggregate fluorescence method. Furthermore, the robust probe also exhibited uncontinuous red fluorescence distribution in cell membranal Lo phase. By taking advantage of this intriguing character, we also successfully showed that the novel probe could be employed to image uncontinuous distribution of cell membranal Lo phase by a 3D imaging technique for the first time. Compared with the conventional cell membrane probes, 1) the **TP-HVC18** not only can visualize membranal Lo phase by an aggregate fluorescence method, 2) but also the probe exhibited uncontinuous red fluorescence distribution in cell membranal Lo phase. 3) In addition, distribution characteristics of Lo phase were intuitively observed by 3D imaging technique.

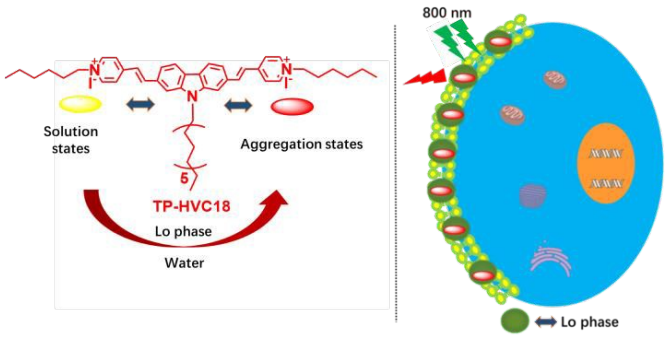

Fig. 1 Structure and imaging method of the new TP probe **TP-HVC18**.

Experimental

Materials

All chemical reagents_were analytical grade. 4,4'-Dibromobiphenyl and 1-bromooctadecane were purchased from Sinopharm Chemical Reagent Co., Ltd (Shanghai, China). DiD, 1,2-dipalmitoyl-*sn*-glycero-3-phosphocholine(DPPC), 1,2-dioleoyl-*sn*-glycero-3- phosphocholine (DOPC), cholesterol (CL), Palladium (II) acetate and tri-o-tolylphosphine were purchased from J&K Chemical (Beijing, China). PBS was purchased from Seikagaku Corporation (Japan). The solvents used in the spectral measurement are of chromatographic grade. TLC analyses were performed on silica gel plates and column chromatography was conducted over silica gel (mesh 200–300), both of which were obtained from Qingdao Ocean Chemicals.

Apparatus

Nuclear magnetic resonance spectra (^{1}H and ^{13}C) were obtained by a Bruker Avanace 300/400 spectrometer. The HRMS spectra were recorded on Agilent Technologies 6510 Q-TOF LC/MS or ThermoFisher LCQ FLEET. The UV-visible-near-IR absorption spectra of dilute solutions were recorded on a Cary 50 spectrophotometer using a quartz cuvette having 1 cm path length. One-photon fluorescence spectra were obtained on a HITACHI F-2700 spectrofluorimeter equipped with a 450-W Xe lamp. Two-photon fluorescence spectra were recorded on a SpectroPro300I. All of confocal microscopic photos were obtained with Carl Zeiss Microscopy LSM780. All of TP microscopic photos were obtained with Olympus FV 300 Laser. The total power was provided by laser source. Dimension Icon scanning electron microscope (SEM) was produced by Veeco Instruments Inc. Transmission electron microscopy (TEM) images were obtained with a JEOL JEM-2100F transmission electron microscope operating at an acceleration voltage of 200 kV.

Cell culture and living cell imaging

SiHa Cancer cells were cultured in Dulbecco's modified Eagle's medium supplemented with penicillin/streptomycin and 10% bovine calf serum in a 5% CO_2 incubator at 37°C. For living cells imaging experiment of **TP-HVC18** (**2 μM**), cells were incubated in culture medium for 20 min at 37 °C, cells images were carried out immediately.

One- and two-photon images of **TP-HVC18** and DiD: Living cells were stained with 2 μM **TP-HVC18** and 4 μM DiD for 40 min and 15 min at ambient temperature, respectively, and then cell images were carried out using one- and two-photon fluorescence microscopy.

Preparation of GUVs

DOPC/CL was used to obtain the giant unilamellar vesicles (GUVs) of liquid-disordered (Ld) phase, while DPPC/CL was used to construct the GUVs of Lo phase. Two GUVs were prepared by the following experimental procedures. Firstly, DOPC (18 mg/mL) and DPPC (18 mg/mL) were dissolved in the mixing solvents of CH_3Cl and CH_3OH (V/V, 2:1). Secondly, both solutions were added to flaskets and fully shocked. Thirdly, the mixed solutions were carefully laid over the inner wall of the flaskets and the solvents were removed under the protection of N_2. Fourthly, to further remove residual solvents, flaskets were treated at vacuum conditions. Finally, the flaskets were filled using 0.1 M sucrose solutions, and further heated at 60^{o}C for 24 h. The GUVs were formed in the sucrose solutions.

Before achieving GUVs confocal imaging, some experiments were prepared. First, we prepared 1 mM stock solution of probes in DMF to stain the GUVs; Second, adding 0.8 mL stock solution to 200 μL glucose solution (0.1 M) and obtained a diluted solution; Third, taking out 10 mL GUVs and adding to the above diluted solution and mixed evenly; Finally, the GUVs confocal imaging were carried out.

Real-color images (*in situ* images) acquirement of GUVs and cells. The laser scanning microscope imaging was carried out by Zeiss LSM 780 confocal fluorescent microscope. The real-color images were acquired by the spectra imaging function of the Zeiss LSM 780 confocal microscope. The above function was capable of separately collecting emission spectra in numerous short wavelength ranges. For example, the images with green color correspond to wavelength of 544-552 nm. The images with the wavelength of 578-586 nm exhibited yellow fluorescence, and the images with the wavelength of 613-621 nm showed red fluorescence, etc. Then the merge of all these images would give a new image and exhibit its real emission spectra, called the real-color image. Meanwhile, management of these images could give the emission intensity at

different wavelength range and further give the *in situ* emission spectra of arbitrary areas.

Preparation of TEM, DLS and SEM

Before achieving TEM experiment, some experiments were prepared. First, we prepared three **TP-HVC18** (4 μM) water/DMF mixtures with different water fraction (f_w), including water/DMF (f_w = 0%), water/DMF (f_w = 75%) and water/DMF (f_w = 100%); Second, taking 10 μL liquid from three water/DMF mixtures to bronze for 20 minutes; Third, absorbing residual liquid with sanitary napkin; Finally, the TEM experiment was carried out. In dynamic light scattering (DLS) experiment, we prepared water/DMF mixtures (f_w = 100%) of **TP-HVC18** (4 μM), and then DLS experiment was carried out. In this work, we use pure solid **TP-HVC18** to achieve SEM experiment.

SEM was produced by Veeco Instruments Inc. Transmission electron microscopy. TEM images were obtained with a JEOL JEM-2100F transmission electron microscope operating at an acceleration voltage of 200 kV.

Synthesis of Probe

Chemical synthesis of **TP-HVC18** was accomplished in a total of five steps (Scheme S1). The optimization of 4,4-dibromo-2-nitrobiphenyl (1) started from readily available 4,4-dibromobiphenyl and nitryl. 2 was steadily prepared as an isolable intermediate for synthesizing 3. 4 was obtained by Heck reaction between 3 and 4-vinylpyridine. Treatment of iodine hexane with 4 in acetone results in the formation of material **TP-HVC18**.

Synthesis of 1 and 2

The compound 1 and 2 was synthesized by literature.[30]

Synthesis of 3.

20 g KOH was added in DMF (70 mL) and the resulting solution was stirred for 30 min. 3.23g (10 mmol) of **2** was then added and the mixture was stirred for another 40 min. Finally, 1-bromooctadecane (4.98 g, 15 mmol) was added dropwise and the mixture reacted for 12 h at room temperature. White solid was found when the mixture was poured into water (500 mL). The crude residue was filtered and washed with ethanol for 3 times. A white solid was obtained for **3** after recrystallization from ethanol with a yield of 80%. ^{1}H NMR (400 MHz, DMSO-*d6*), δ (ppm): 7.89 (d, *J* = 8.28 Hz, 2H), 7.58 (d, *J* = 1.40 Hz, 2H), 7.35 (dd, *J1* = 8.26 Hz, *J2* = 1.54 Hz, 2H), 7.26 (s, *2*H), 4.19 (t, *J* = 7.34 Hz, 2H), 1.84 (t, *J* = 7.14 Hz, 2H), 1.25-1.34 (m, 30 H), 1.25 (t, *J* = 6.80 Hz, 3H).

Synthesis of 4

The compound **3** (4.60 g, 8.0 mmol) was added into a flask containing a mixture of palladium(II) acetate (0.18 g, 0.8 mmol), tri-*o*-tolylphosphine (0.72 g, 2.4 mmol) and K_2CO_3 (8.8 g, 64.0 mmol), and to this mixture *N*-methyl-2-pyrrolidone (NMP, 40 mL) and 4-vinylpyridine (3.4 g, 32.0 mmol) was added. The system was heated to 128 °C for 3 days under the protection of argon. A dark-red suspension was obtained. When the resulting mixture was cooled to room temperature, it was poured into H_2O (500 mL) and extracted with CH_2Cl_2. Then the organic phases were separated, the excess organic solvent was removed by vacuum distillation and a dark-red solution was obtained. The title product was obtained as a yellow solid after the residue was recrystallized from ethanol (yield: 50%). ^{1}H NMR (400 MHz, DMSO-*d6*) δ (ppm): 8.61 (d, *J* = 5.44 Hz, 4H), 8.08 (d, *J* = 8.08 Hz, 2H), 7.49-7.58 (m, 10H), 7.15-7.26 (m, 2H), 4.37 (t, *J* = 7.20 Hz, 2H), 1.94 (t, *J* = 7.16 Hz, 4H), 1.23 (s, 28H), 0.87 (t, *J* = 6.82 Hz, 3H).

Synthesis of TP-HVC18

The compound 4 **(**1.25 g, 2 mmol) and excess 1-iodododecane were dissolved in acetone and stirred for 2 h at room temperature. Then the mixture was refluxed for another 12 h and a red residue was obtained. The residue was filtered and then washed with methanol for 3 times. The title product was obtained as a red solid after the residue was recrystallized from ethanol (Yield: 75%). ^{1}H NMR (300 MHz, DMSO-*d6*), δ (ppm): 8.97 (d, *J* = 6.90 Hz, 4H), 8.22–8.33 (m, 8H), 8.08 (s, 2H), 7.71 (t, *J* = 8.80 Hz, 2H), 7.67 (s, 2H), 4.50 (t, *J* = 7.20 Hz, 2H), 1.91 (d, *J* = 6.00 Hz, 6H),1.15-1.31 (m, 42H), 0.81-0.90 (m, 9H). ^{13}C NMR (100 MHz, DMSO-*d6*): δ 152.95, 144.12, 141.99, 141.26 133.53, 123.58, 123.47, 122.78, 121.30, 119.32, 109.75, 59.61, 31.17, 30.48, 30.40, 28.90, 28.87, 28.77, 28.66, 28.57, 28.48, 26.37, 25.10, 21.96. HRMS (m/z): $[M-I]^+$calcd for $C_{56}H_{81}I_2N_3$, 397.8200; found, 397.8213.

Results and discussion

Optical properties of TP-HVC18

With **TP-HVC18** in hand, we set out to investigate optical properties of the **TP-HVC18** in various solvents. As shown in Fig. S1 and Table S1 (ESI†), in pure water solution, the compound **TP-HVC18** has maximal absorption and emission at 429 nm and 612 nm, respectively; In DMF solution, **TP-HVC18** has maximal absorption and emission at 447 nm and 555 nm, respectively. The results demonstrated that **TP-HVC18** exhibited larger Stokes shift in aqueous solution than organic solution. Moreover, the red solid **TP-HVC18** showed strong red fluorescence signal at wide-field excitation (Fig. S2, ESI†). Thus, we envisioned that red emission signal of **TP-HVC18** may come from aggregation of compound in pure water system.

We further investigated TP properties of **TP-HVC18** in aqueous solution. As shown in Table S2 (ESI†), the compound **TP-HVC18** possessed large TP action absorption cross-section ($\delta\Phi$) in pure water system and buffer solution. The results demonstrated that the **TP-HVC18** should be a novel TP fluorescent material. Thus, we deduced that the compound **TP-HVC18** may be a novel TP probe with aggregate fluorescence property.

Aggregation of TP-HVC18

To verify the compound **TP-HVC18** could aggregate in aqueous solution, we investigated optical properties of **TP-HVC18** in the distinct polar environments. We have proved that red solid **TP-HVC18** emitted strong red fluorescence at wide-field excitation. Thus, the compound **TP-HVC18** may form red nanoribbon in water/DMF mixtures with a high water fraction (f_w).

To prove the above assumption, we investigated optical properties of **TP-HVC18** in water/DMF mixtures. First, we prepared eight water/DMF mixtures of **TP-HVC18**; Under ultraviolet lamp, the compound **TP-HVC18** exhibited bright yellow fluorescence in organic solutions, however, fluorescence signal gradually became

red with increasing f_w values (Fig. 2A). Second, we measured one- and two-photon emission spectra of **TP-HVC18** in different water/DMF mixtures. When f_w increased from 0 to 100 %, the one- and two-photon fluorescent spectra underwent red shift (Figs. 2B-C), however, fluorescent intensity of **TP-HVC18** decreased gradually (Figs. 2D-E). Moreover, the fluorescence spectrum of **TP-HVC18** in pure water solution was consistent with solid fluorescence of **TP-HVC18** (Fig. 2F). The above results demonstrated that **TP-HVC18** displayed two different fluorescence emission profiles to the aggregate and solution states. Thus, we induced **TP-HVC18** should have unique morphology in definite f_w values.

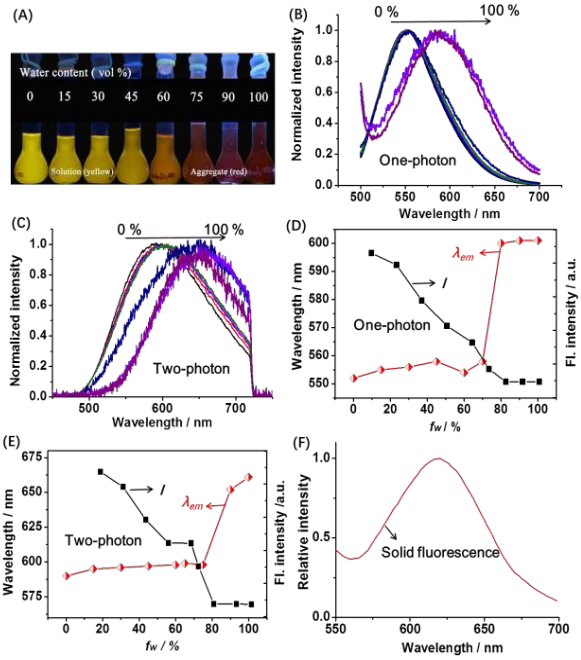

Fig. 2 (A) Photographs of **TP-HVC18** in water/DMF mixtures; (B) One- and (C) two-photon fluorescence spectra of **TP-HVC18** in water/DMF mixture; Plots of maximum (D) one- and (E) two-photon emission intensity (I) and wavelength (λ_{em}) of **TP-HVC18** versus water/DMF (f_w, vol %) in water/DMF mixtures; (F) Solid fluorescence spectra of **TP-HVC18**. **[TP-HVC18]** = 4 μM. λ_{ex} = 488 nm.

Investigating aggregation of TP-HVC18 by SEM, DLS and TEM techniques

We further investigated aggregation of **TP-HVC18** by scanning electron microscope (SEM), dynamic light scattering (DLS) and transmission electron microscopy (TEM). First, we observed morphology of the solid **TP-HVC18** by SEM. As shown in Fig. 3A, the red solid **TP-HVC18** aggregated and formed nanoribbon with different length and width; Second, as shown in Fig. 3B, it was found that **TP-HVC18** could not occur aggregation in pure orgnic solvent; We prepared **TP-HVC18** water/DMF (f_w = 75%) solution, and then TEM experiment was carried out. Similarly with SEM experiment, imaging results exhibited nanoribbon with different length and width (Fig. 3C); Furthermore, the dye **TP-HVC18** further formed irregular aggregation in pure water solution (Fig. 3D). Finally, we further investigated size of **TP-HVC18** in pure water system by DLS technique. Similarly with SEM and TEM, DLS in water/DMF (f_w = 100 %) highlighted irregular nanoribbon with an average size of 10-600 nm (Fig. 3E). The results of SEM, TEM and DLS techniques were consistent with optical properties of **TP-HVC18** in different f_w values. The above results further demonstrated that **TP-HVC18** was a novel fluorescent material with aggregate fluorescence feature. We predicted that **TP-HVC18** should possess unique applications by an aggregate fluorescence method.

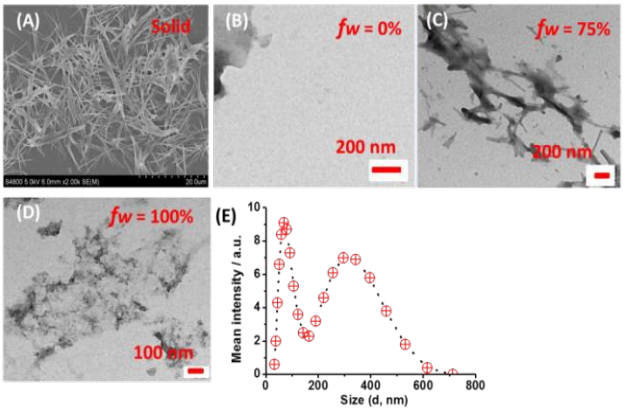

Fig. 3 (A) SEM picture of the solid **TP-HVC18**; (B) TEM pictures of water/DMF (f_w = 0%), (C) water/DMF (f_w = 75%) and (D) water/DMF (f_w = 100%) dispersions of **TP-HVC18** at 4 μM; (E) DLS of **TP-HVC18** dispersions in water/DMF (f_w = 100 %) mixtures at 4 μM.

In situ imaging

We further investigated **TP-HVC18** whether possessed unique applications *in vitro* and *in vivo*. According to previous studies on the physical properties of model membranes, giant unilamellar vesicles (GUVs) were powerful tools to simulate cell membrane.[31] DOPC/CL can construct cell membranal liquid-disordered (Ld) phase, while DPPC/CL can simulate cell membranal Lo phase.[32-35] We have proved that fluorescence spectra of **TP-HVC18** exhibited yellow and red fluorescence emission in solution and aggregation state (Fig. 4A); Next, fluorescence spectra of **TP-HVC18** in Lo and Ld phases solutions were also measured (Fig. 4B). Interestingly, in accordance with its aggregate properties, **TP-HVC18** also can emit red fluorescence signal in Lo phase solution. Thus, we envisioned that the probe **TP-HVC18** could sense cell membranal Lo phase by an aggregate fluorescence method.

To prove the above assumptions, we further investigated *in situ* imaging of GUVs. Real-color images of GUVs stained with **TP-HVC18** were acquired (Figs. 4C and D). The *in situ* imaging showed that **TP-HVC18** emitted yellow and red fluorescence in Lo and Ld phase, respectively. *In situ* imaging results GUVs were consistent with fluorescence emission of **TP-HVC18** in Lo and Ld phases solutions. Thus, the **TP-HVC18** should form aggregation states in Lo phase and emit red fluorescence signal. We further proved that the probe was capable of imaging GUV of Lo phase by an aggregate fluorescence method.

To prove the probe **TP-HVC18** can imaging SiHa cell membranal Lo phase, the cell membranal *in situ* imaging experiment was carried out. The toxicity test indicated that the **TP-HVC18** had low toxicity for living cells (Fig. S3, ESI†). The cell membranes imaging and *in situ* emission profiles of the **TP-HVC18** were displayed in Figs. 4E-G and Fig. S4 (ESI†). The *in situ* imaging result demonstrated that

TP-HVC18 emitted red fluorescence signal in the cell membranes at 488 nm excitation (Fig. 4F). This result was similar with fluorescence characteristics of Lo phase. Furthermore, the *in situ* emission spectrum of the cell membrane was consistent with solid fluorescence of **TP-HVC18** (Fig. 4G). The results demonstrated that the **TP-HVC18** was suitable for imaging membranal Lo phase by an aggregate fluorescence method.

We have demonstrated that **TP-HVC18** displayed red and yellow fluorescence emission profiles to the Lo and Ld phases. However, it cannot find yellow fluorescence signal of Ld phase in cell membranes. Thus, we set out to investigate *in situ* imaging of Ld phase by changing experiment condition. Living SiHa cells were incubated with 1 μM **TP-HVC18** for a long time (about 1.5 h). As shown in Fig. 5, the *in situ* imaging result exhibited red and yellow fluorescence signal in the cell membranes (Fig. 5A), in good agreement with *in site* imaging of GUVs. The *in situ* emission spectra of the cell membranes were consistant with the *in situ* emission profiles of both vesicles solutions (Fig. 4B). The results showed that **TP-HVC18** can image cell membranal Lo and Ld phases based on two different sets of fluorescence signals.

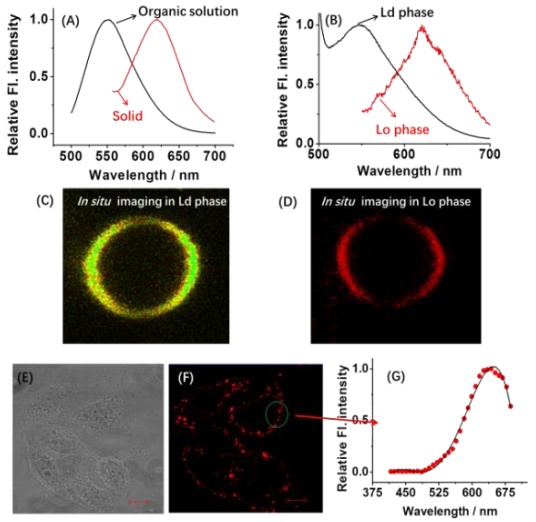

Fig. 4 (A) Fluorescence spectra of **TP-HVC18** in organic solution, and solid fluorescence of **TP-HVC18**; (B) Fluorescence spectra of **TP-HVC18** (2 μM) in various vesicle solutions; (C) *In situ* image of Lo phase GUVs incubated with **TP-HVC18** (2 μM); (D) *In situ* image of Ld phase GUVs incubated with **TP-HVC18** (2 μM); (E) Bright-field images; (F) *In situ* emission spectra of the cell membranes incubated with **TP-HVC18** (2 μM). λ_{ex} = 488 nm. Bar = 20 μm.

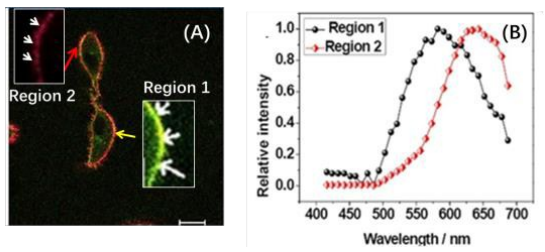

Fig. 5 (A) Fluorescence images and spectra of the SiHa cells incubated with **TP-HVC18** (1 μM) using the spectra imaging function of the Zeiss LSM 780 confocal fluorescent microscope. (B) Fluorescence spectra of the SiHa cells with excitation at 488 nm. Scale bar = 20 μm.

Aggregation of TP-HVC18 in cell membranal Lo phase

To further demonstrate **TP-HVC18** can label membranal Lo phase by an aggregate fluorescence method, we further study imaging characteristics of the **TP-HVC18** in the cell membranes. As shown in Figs. 6A-C, the **TP-HVC18** presented uncontinuous red fluorescence distribution in the cell membranes at 488 nm excitation. Moreover, aggregation fluorescence signal was also observed at 800 nm excitation (Figs. 6D-F). To obtain fluorescence intensity profile of Lo phase, we chose a SiHa cell (Fig. 6B) and investigated fluorescence distribution in the cell membranes; The intensity profile of linear regions of interest across SiHa cell exhibited uncontinuous fluorescent intensity (Fig. 6G). This result further demonstrated the probe **TP-HVC18** could label cell membranal Lo phase by an aggregate fluorescence method. To the best of our knowledge, no reports to date have been published on fluorescent probes with aggregate fluorescence property for visualizing membranal Lo phase using one- and two-photon microscope.

Conventional membrane probes could not visualize membranal Lo phase based on aggregate fluorescence method. To prove this point, we chose the commercially available membrane tracer DiD to investigate its one- and two-photon images. Before studying cells membrane imaging, We firstly study optical properties of DiD in the distinct polar environments. The results demonstrated that fluorescence of DiD gradually quenching when f_w increased from 0 to 100% (Fig. S5, ESI†). Thus, we envisioned that the commercially probe DiD could not image cell membanal Lo phase by an aggregate fluorescence method.

We further investigated cell membranes imaging of DiD. Living cells were incubated with 2 μM DiD for 15 min at room temperature, and then one- and two-photon imaging experiment were carried out. As shown in Figs. 6H-I, the DiD presented continuous fluorescence distribution in the cell membranes; This imaging characteristics were intuitively observed by 3D imaging technique (Fig. 6J). Compared to **TP-HVC18**, the probe DiD cannot image cell membranes at 800 nm excitation (Figs. 6K-M). The intensity profile of linear regions of interest across a SiHa cell further proved continuous fluorescence distribution of DiD (Fig. 6N). The above results demonstrated that DiD cannot detect membranal Lo phase at OP and TP excitation. The confocal image of **TP-HVC18** did not merge well with that of the DiD. Moreover, the Pearson's colocalization coefficient is only 0.40, demonstrating that DiD and **TP-HVC18** cannot locate in the same region (Fig. S6, ESI†).

Compared to commercial membrane probe DiD, the **TP-HVC18** not only can visualize membranal Lo phase at one- and two-photon excitation, but also the probe exhibited uncontinuous red fluorescence distribution in cell membranal Lo phase. In addition, the **TP-HVC18** showed higher photostability (Fig. S7, ESI†) than DiD (Fig. S8, ESI†).

3D imaging

To further demonstrate the probe **TP-HVC18** was capable of imaging cell membranal Lo phase by an aggregate fluorescence method, 3D imaging experiment was carried out**.** Firstly, SiHa cells were incubated with 2 μM **TP-HVC18** for 40 min, and further did tomoscan experiment. 15 optical sections of cells at different depths have been recorded (Fig. 7A). The image results exhibited distribution characteristics of Lo phase at different depths. Secondly,

View Article Online
DOI: 10.1039/C7TB00979H

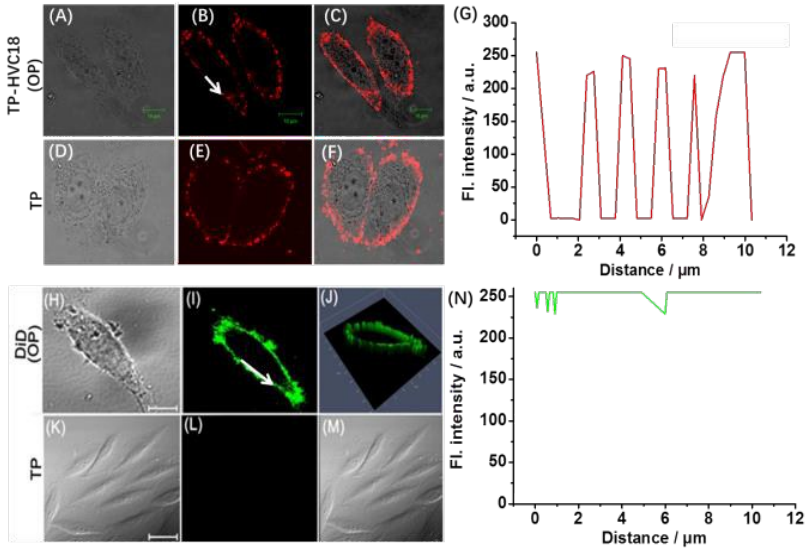

Fig. 6 One- and two-photon images of the cell membranes treated with **TP-HVC18** (2 μM) and DiD (2 μM). (A) Bright-field image. (B) One-photon image of the cell membranes treated with **TP-HVC18** (2 μM); λ_{ex} = 488 nm, λ_{em} = 675-700 nm. (C) Merged image of A and B. (D) Bright-field image. (E) Two-photon image of the cell membranes treated with **TP-HVC18** (2 μM); λ_{ex} = 800 nm, λ_{em} = 675-700 nm. (F) Merged image of D and E; (G) Intensity profile of the region of interest (white arrow in B) across the SiHa cells (B). (H) Bright-field image. (I) One-photon image of the cell membranes treated with DiD (2 μM); λ_{ex} = 633 nm, λ_{em} = 635-691nm. (J) 3D image of I; (K) Bright-field image; (L) Two-photon image of the cell membranes treated with DiD (2 μM); λ_{ex} = 800 nm, λ_{em} = 675-700 nm. (M) Merged image of K and L. (N) Intensity profile of the region of interest (white arrow in I) across the SiHa cells.

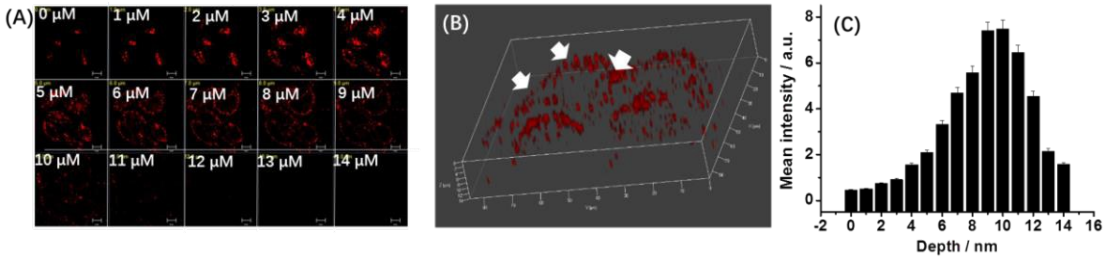

Fig. 7 (A) Confocal imaging of **TP-HVC18** including 15 optical sections at different depths has been recorded.(B) Confocal 3D imaging of **TP-HVC18** including 15 optical sections ; (C) Changes of fluorescent intensity of **TP-HVC18** in cell membrane at different depths. λ_{ex} = 488 nm. λ_{em}= 650-700 nm.

to intuitive observe aggregation of probe in the cell membranes, 3D imaging was obtained by Nikon AIMP analysis software (Fig. 7B). It successfully showed that the novel probe **TP-HVC18** can be employed to exhibit uncontinuous distribution of cell membranal Lo phase. In addition, the intensity profile of every pictures constituting 3D imaging was acquired. Cell membranal fluorescence intensity enhanced gradually in the range of 0-10 μm; Furthermore, fluorescence signal further weaken within the range of 10-14 μm (Fig. 7C). Thus, by taking advantage of the above character, it was firstly found that **TP-HVC18** can be employed to image uncontinuous distribution of cell membranal Lo phase by 3D imaging technique for the first time.

Conclusions

In summary, we have developed a novel TP fluorescent probe **TP-HVC18** based on the 2,7-position substituted carbazole derivative. The new probe displayed two different fluorescence emission profiles to aggregate and solution states. Similarly with its optical properties of aggregate state, **TP-HVC18** remarkably displayed red fluorescence emission signal in the Lo phase vesicles. View of this property, **TP-HVC18** can image cell membranal Lo phase by an aggregate fluorescence method. Furthermore, the robust probe also exhibited uncontinuous red fluorescence distribution in cell membranal Lo phase. By taking advantage of this intriguing character, it was found that the novel TP probe **TP-HVC18** was capable of visualizing membranal Lo phase by a 3D imaging technique. We expect that this fluorescent platform might be extended for the development of a wide variety of functional probes for detecting intracellular phase states.

Acknowledgements

This work was financially supported by NSFC (21472067, 21672083, 51503077), Taishan Scholar Foundation (TS 201511041), and the

startup fund of the University of Jinan (309-10004). Doctor start up fund of University of Jinnan (160082102) and NSFSP (ZR2015PE001).

Notes and references

1 R. P. Haugland, The handbook, *A Guide to Fluorescent Probes and Labeling Technologies*, ed. M. T. Z. Spence, 10th ed., 2005, pp. 710.

2 J. R. Lakowicz, *Principles of fluorescence spectroscopy*. Springer: New York, NY, 2006.

3 B. Valeur, N. M. Berberan-Santos, *Molecular Fluorescence: Principles and applications.*2nd ed. Wiley: Germany, 2012.

4 J. Luo, Z. Xie, J. W. Y. Lam, L. Cheng, H. Chen, C. Qiu, H. S. Kwok, X. Zhan, Y. Liu, D. Zhu and B. Z. Tang, *Chem. Commun.*, 2001, 1740.

5 R. Hu, N. L. C. Leung and B. Z. Tang, *Chem. Soc. Rev*., 2014, **43**, 4494.

6 X. Yan, T. R. Cook, P. Wang, F. Huang and P. J. Stang, *Nat. Chem*. 2015, **7**, 342.

7 J. W. Y. Lam and B. Z. Tang, *Chem. Rev.*, 2009, **109**, 5799.

8 Y. Hong, J. W. Y. Lam and B. Z. Tang, *Chem. Soc. Rev*., 2011, **40**, 5361-5388.

9 W. Denk, J. H. Strickler and W. W. Webb, *Science*, 1990, **248**, 73.

10 Y. Park, K. T. Lee, Y. D. Suh, and T. Hyeon, *Chem. Soc. Rev*., 2015, **44**, 1302.

11 X. Wang, A. R. Morales, T. Urakami, L. Zhang, M. V. Bondar, M. Komatsu and K. D. Belfield, *Bioconjugate. Chem*., 2011, **22**, 1438.

12 Sherwood, L. *Human Physiology: From cells to systems*, New York: West Publishing Company. 1993.

13 H. Lodish, A. Berk, S. L. Zipursky, P. Matsudaira, D. Baltimore and J. Darnell, *Molecular Cell Biology*. New York, Scientific American Book, 4th ed., 2004.

14 B. Nichols, *Nature*, 2005, **436**, 638.

15 P. J. Fraker and J. C. Speck Jr., *Biochem. Bioph. Res. Co*., 1978, **80**, 849.

16 P. L. Yeagle, *Biochim. Biophys. Acta.*, 1985, **822**, 267.

17 S. L. Singer and G. L. Nicolson, *Science*, 1972, **175**, 720.

18 K. Bacia, P. Schwille and T. Kurzchalia, *Proc. Natl. Acad. Sci. USA.*, 2005, **102**, 3272.

19 J. J. Hanand and D. W. Boo, *Langmuir.*, 2009, **25**, 3083.

20 R. Welti, D. A. Rintouli, F. Goodsaid-Zalduondo, S. Felder and D. F. Silb, *J. Biol. Chem*., 1981, **256**, 7528.

21 T. P. W. McMullen, R. N. A. H. Lewis, R. N. McElhaney, *Curr. Opin. Colloid. Interface. Sci*., 2004, **8**, 459.

22 E. W. Steckel, B. E. Welbaum and J. M. Sodetz, *J. Biol. Chem.*, 1983, **258**, 4318.

23 A. Sergé, N. Bertaux, H. Rigneault and D. Marguet, *Nat. Methods.*, 2008, **5**, 687.

24 Y. Okimoto, A. Watanabe, E. Niki, T. Yamashita and N. Noguchi, *FEBS. Lett*., 2000, **474**, 137.

25 Y. Okimoto, A. Watanabe, E. Niki and T. Yamashita, N. Noguchi, *Science*, 1977, **195**, 307.

26 E. I. Goksu, J. M. Vanegas, C. D. Blanchette, W. C. Lin and M. L. Longo, *Biochim. Biophys. Acta*., 2009, **1788**, 254.

27 S. M. Potter, *Curr. Biol.*, 1996, **6**, 1595.

28 V. E. Centonze and J. G. White, *Biophys. J.*, 1998, **75**, 2015.

29 F. Helmchen and W. Denk, *Nat. Methods*., 2005, **2**, 932.

30 Y. Liu, F. Meng, L. He, X. Yu and W. Lin, *Chem. Commun.*, 2016, **52**, 8838.

31 M. D. Molin, Q. Verolet, A. Colom, R. Letrun, E. Derivery, M. Gonzalez-Gaitan, E. Vauthey, A. Roux, N. Sakai and S. Matile, *J. Am. Chem. Soc.*, 2015, **137**, 568.

32 F. Aresta-Branco, A. M. Cordeiro, H. S. Marinho, L. Cyrne, F. Antunes and R. F. M. de Almeida, *J. Biol. Chem.*, 2011, **279**, 5043.

33 B. Pawlikowska-Pawlęga, L. E. Misiak, B. Zarzyka, R. Paduch, A. Gawron and W. I. Gruszecki, *Biochim. Biophys.*, 2012, **1818**, 1785.

34 B. Ramstedt and J. P. Slotte, *Biochim. Biophys. Acta*., 2006, **1758**, 1945.

35 T. –Y. Wang, and J. R. Silvius, *Biophys. J*., 2000, **79**, 1478.

View Article Online
DOI: 10.1039/C7TB00979H

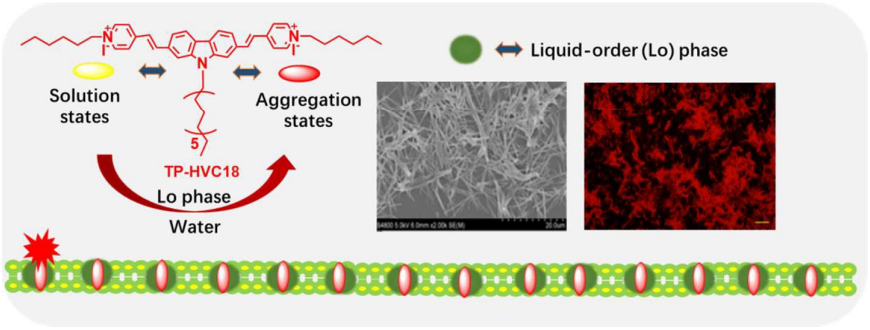

In this work, we have engineered a novel two-photon fluorescent probe, **TP-HVC18**, which remarkably displayed two different fluorescence emission profiles to the aggregate and solution states in the distinct polar environments. Taking advantage of this unique feature, we have demonstrated that the new TP probe **TP-HVC18** was suitable for imaging membranal Lo phase by an aggregate fluorescence method.